



## Effect of Treatment Processes on the Morphology and Mechanical Properties of Natural Fiber-Reinforced Epoxy Composites

T.O. Ogundana<sup>1</sup>, B.O. Bolaji<sup>1</sup>, O.T. Oginni<sup>2</sup>, F.A. Onuh<sup>1</sup>, I.A. Olumoroti<sup>1</sup>, M.O. Olagunju<sup>2</sup>

<sup>1</sup>Department of Mechanical Engineering, Federal University Oye-Ekiti, Nigeria.

<sup>2</sup>Department of Mechanical Engineering, School of Engineering Technology, Bamidele Olumilua University of Education, Science and Engineering Ikere-Ekiti, Nigeria.

Corresponding author: [tunde.ogundana@fuoye.edu.ng](mailto:tunde.ogundana@fuoye.edu.ng) (Ogundana T.O)

### Article History

Received: 10-02-25  
Revised: 28-02-25  
Accepted: 10-03-25  
Published: 25-03-25

### Abstract

The automotive industry is incorporating sustainable materials like rice husk into interiors for affordability, biodegradability, low density, and enhanced properties like durability and corrosion resistance. This research developed and characterized coir fibre and rice husk-reinforced epoxy composites, evaluating their mechanical, thermal, and water absorption properties. Coir fibres and rice husks were extracted, washed, sun-dried, and treated with sodium hydroxide, creating composites. The composites were tested for tensile strength impact resistance, water absorption, and thermal stability using Thermogravimetric analysis, Fourier Transform Infrared Spectrometry, Scanning Electron Microscope, and Izod impact testing for characterization. Rice husk (RH) composites exhibit increased water absorption at smaller particle sizes (425 µm and 600 µm), coir composites show enhanced absorption at larger sizes (1180 µm), and coir/RH blend composites maintain consistent water absorption. Untreated coir and RH composites showed higher impact energy at 425 µm, with smaller particle sizes being more effective for reinforcement, with 425 µm being the optimal size. The treatment improved water absorption in RH composites, particularly coir composites, with the highest absorption at 1180 µm, and also enhanced their impact resistance. The study reveals that treated coir fibre composites improve tensile strength, thermal stability, and impact resistance, while RH composites enhance impact resistance with varying particle sizes. Coir/RH blend composites, which balance water absorption and heat treatment, are highly beneficial in various industries such as automotive, aerospace, oil and gas, marine, and construction.

**Keywords:** Composites; sustainable materials; impact energy; water absorption; thermal stability

### 1. Introduction

Humanity has utilized materials for various purposes throughout history, with technological advancements based on engineering materials. The need for ecological sustainability has grown, leading to efforts to create energy-efficient, sustainable composite materials. This is in response to the growing global demand for renewable and eco-friendly products (Choi et al., 2023; Ganasan et al., 2024). Composite materials combine two materials for strength, lightweight, durability, design flexibility, and corrosion resistance. They have a significant impact on human history, serving in various industries like construction, automotive, aeronautics, and household fittings. Benefits include strength, lightweight, durability, design flexibility, and corrosion resistance (Faheed, 2024). Research in composite materials aims to replace traditional materials in engineering applications by blending components' properties for superior materials (Wang et al., 2024).

Reinforcements, such as fibers, flakes, and particles, enhance the durability and adaptability of composite materials. Fibres are the most commonly used reinforcements or composite materials, influencing their characteristics and being recognized for their environmental sustainability and adaptability compared to traditional synthetic fiber composites (Ahmed et al., 2023; Akter et al., 2024). Composite materials, with high aspect ratio fibers, are versatile in automotive, aerospace, and construction industries. They can be reinforced with various fibres like boron, aramid, glass, carbon, and natural fibers (Chichane et al., 2023; Nasri et al., 2024).

Natural fibers, derived from plants, minerals, or animals, are gaining attention as cost-effective, renewable, and low-density alternatives to synthetic materials, offering energy savings and suitability for lightweight applications (Mohan and Kanny, 2023; Kiruthika, 2024). Natural plant-derived fibers offer low manufacturing temperatures, design flexibility, pollution-free production, and cost-effectiveness. Primarily composed of cellulose, addressing environmental and health risks in polymer matrices (Shaaban et al., 2024). Researchers are exploring the use of natural fibers in reinforcing polymers for their superior formability, renewable nature, cost-effectiveness, eco-friendliness, and applications in engineering (Sanjay et al., 2016).

Natural fibers like coir, rice husk, and flax are being used in composites due to their eco-friendly properties, but their strength is limited in non-bearing applications (Santos et al., 2024). Composite materials are gaining popularity in automotive and aerospace due to their superior strength, stiffness, and lightweight design, with fiber-reinforced composites outperforming traditional materials (Sharma et al., 2020; Sakti, 2024). The dashboard, a vital automotive component, can be made eco-friendly, lightweight, and long-lasting using

natural reinforced fibers like coir and rice husk, thereby reducing the automotive sector's environmental footprint. Composite materials offer numerous advantages such as high strength, low weight, corrosion resistance, low densities, thermal and electrical conductivities, energy absorption, and aesthetic color effects (Patel et al., 2018). Composite materials offer weight savings, stiffness, and strength. The matrix, made of polymers, metals, ceramics, and carbon, influences the composite's properties and behavior.

The automotive industry is embracing sustainability by exploring natural and renewable materials like coir and rice husk for composite reinforcement, aiming to enhance fuel efficiency and vehicle performance. The industry is exploring sustainable, lightweight materials like coir and rice husk composites for dashboards, focusing on thermal stability and environmental benefits. The mechanical properties of composite materials are influenced by the type of fiber used, with fibrous composites enhancing toughness and resistance to deformation. Chemical treatment, increased interfacial bonding between matrix and reinforcement, and the use of rice husk and rice ash can improve their performance (Oyiborhoro et al., 2024; Umma, 2022).

These materials are derived from natural and renewable resources like cotton, wool, silk, cellulose, hemp, flax, coir, and rice husk. Rice husk's high silica content makes it a valuable resource for various industrial applications. Researchers are exploring its potential as a filler in polymer composites to solve waste disposal issues (Abhishe and Mrutyunjaya, 2016). It's used in various industries, with alkaline treatment (Valasek et al., 2021; Gil-Sánchez et al., 2021).

Reviewed literature lacks the effects of fiber treatment and epoxy matrix formulation on thermal stability, moisture absorption, degradation mechanisms, surface morphology, and interface properties for automotive applications using coir and rice husk. Coir and rice husk, abundant agricultural by-products, could be explored as a cost-effective alternative to traditional automotive dashboard materials, enhancing their economic feasibility.

This study investigates the impact of particle sizes and treatment on coir's mechanical properties, aiming to enhance composite materials for automotive applications. It assesses the environmental impact of composites, focusing on production processes, recyclability, and sustainability, thereby enhancing sustainable practices in the automotive industry.

### 2. Materials and Method

#### 2.1 Sample Preparation

Coconut fibers (CF) were extracted from the husk, washed with clean water to remove impurities and dirt, and sun-dried for three days to produce coir. The coir samples were prepared by cutting the coir into smaller pieces for easy grinding.

The coir was ground and divided into two parts, then treated with 0.4% sodium hydroxide solution for eight hours, washed with water, and sun-dried for two days. The second half of the coir was oven dried at 60°C for 4 hours, then cooled to room temperature and stored in an airtight container to prevent moisture absorption. The rice husk (RH) was obtained from the rice milling sector in Ikole Ekiti, Nigeria. After washing with deionized water, the sample was sun-dried for three days. The rice husk was then ground using a grinding machine, producing fibers of varying lengths. The fiber sizes were separated using a sieve shaker with different sieves

## 2.2 Samples Treatment

Coir and rice husk (RH) fibers underwent chemical treatment with 0.4% sodium hydroxide (NaOH). Chopped coir fibers (5–10 mm) were dried, washed, immersed in NaOH for eight hours, rinsed with distilled water, and dried at room temperature for five days to remove moisture. The process was repeated for both coir and RH fibers. The samples were then sieved using three sieve sizes (1180 µm, 600 µm, and 425 µm) to determine particle size.

## 2.3 Composite Production

Composites were prepared using hand layup according to ASTM E1131 standard, with test specimens made with varying coir fiber and RH weights. The fiber samples and epoxy were weighed, mixed, and stirred until homogenous. Half of the hardener (by weight) was added and stirred for another two minutes. The composites were coated with a releasing agent on the inner surface of a mold to prevent sticking. The mixture was then poured into the mold and allowed to cure for 24 hours before removal.

## 2.4 Composition formulation and casting

The sieving process used sieve sizes A (0–425 µm), B (426–600 µm), and C (601–1180 µm). Composite production for sieve sizes A, B, and C using treated coir and rice husk (RH) was investigated. The epoxy mass was varied with coir to achieve a total weight of 100 g. Tables 1 to 6 present the composite formulations for both treated and untreated samples across different sieve sizes.

Table 1: Treated coir and RH with sieve size A (Formulations A)

Sample	Epoxy	Coir	RH
A1	95	5	-
A2	90	10	-
A3	95	-	5
A4	90	-	10
A5	95	2.5	2.5
A6	90	5	5
A7(control value)	100	-	-

Table 2: Treated coir and RH with sieve size B (Formulations B)

Sample	Epoxy	Coir	RH
B1	95	5	-
B2	90	10	-
B3	95	-	5
B4	90	-	10
B5	95	2.5	2.5
B6	90	5	5
B7(control value)	100	-	-

Table 3: Treated coir and RH with sieve size C (Formulations C)

Sample	Epoxy	Coir	RH
C1	95	5	-
C2	90	10	-
C3	95	-	5
C4	90	-	10
C5	95	2.5	2.5
C6	90	5	5
C7(control value)	100	-	-

Table 4: Untreated coir and RH with sieve size A (Formulations D)

Sample	Epoxy	Coir	RH
D1	95	5	-
D2	90	10	-
D3	95	-	5
D4	90	-	10
D5	95	2.5	2.5
D6	90	5	5
D7 (control value)	100	-	-

Table 5: Untreated coir and RH with sieve size B (Formulations E)

Sample	Epoxy	Coir	RH
E1	95	5	-
E2	90	10	-
E3	95	-	5
E4	90	-	10
E5	95	2.5	2.5
E6	90	5	5
E7 (control value)	100	-	-

Table 6: Untreated coir and RH with sieve size C (Formulations f)

Sample	Epoxy	Coir	RH
F1	95	5	-
F2	90	10	-
F3	95	-	5
F4	90	-	10
F5	95	2.5	2.5
F6	90	5	5
F7 (control value)	100	-	-

## 2.5 Experimental Test

Thermogravimetric analysis (TGA) was performed using a DTG-60H SHIMADZU analyzer to assess thermal stability and weight loss over specific temperature ranges, in accordance with ASTM E1131. Fourier transform infrared spectrometry (FTIR) analysis was performed utilizing infrared spectrometry to evaluate biomineral content in isolated samples, identifying compounds and determining material quality. The process optimizes processing conditions and predicts final product performance. The impact test (IT) conducted assessed the impact resistance of composite materials, crucial for industrial applications, particularly automotive, according to ASTM D7066/D7066M standard method. The specimen was impacted at a velocity of 5 m/s with an impact energy of 50 J. The tensile test (TT): TT conducted in accordance with ASTM D7565M-10(2017), assessed the strength of fiber-reinforced polymer matrix composite bars at a constant tensile load of 2 mm/min with a maximum length of 80 mm for industrial applications. Water Absorption Test (WAT): WAT was performed to assess the water absorption capacity of the composites. The test involved cutting and drying samples, recording their initial weight ( $W_1$ ) in grams, submerging them in distilled water at room temperature, and removing them at specific intervals of 12 hours. The samples were dried, their weight recorded ( $W_2$ ), and the procedure repeated for all tested samples. The water absorption percentage was calculated using Equation 1

$$W_a = \frac{W_2 - W_1}{W_1} \times \% \quad (1)$$

## 3. Results and Discussion

The results of impact energy values of treated RH composites were observed to be lower than untreated composites for all particle sizes, decreasing with particle size from 425 µm to 600 µm, then increasing at 1180 µm as presented in Figures 1 and 2. The smaller particle sizes (425 µm and 600 µm) reduce impact energy more than larger ones, suggesting 425 µm may be optimal for maximizing impact energy (Figure 1). Untreated RH composites exhibit higher impact energy values for all particle sizes, suggesting that treatment decreases the material's toughness. The study reveals that the treatment process decreases the impact energy of rice husk composites, with smaller particle sizes resulting in higher energy values. The optimal particle size is 425 µm for both treated and untreated composites.

The treatment process enhances the impact energy of coir composites at a 600  $\mu\text{m}$  particle size but reduces it at 425  $\mu\text{m}$  and 1180  $\mu\text{m}$ , while untreated composites show a different trend (Figure 2). The study reveals that coir composites' impact energy is significantly improved at 600  $\mu\text{m}$  particle size, while untreated composites prefer 1180  $\mu\text{m}$ , highlighting the significant impact of particle size. Figure 3 reveals that treatment of coir/RH composites significantly enhances their impact energy at particle sizes 425  $\mu\text{m}$  and 1180  $\mu\text{m}$ , with the highest values recorded at these sizes. The study shows that coir/RH composite treatment enhances impact energy, particularly at particle sizes 425  $\mu\text{m}$  and 1180  $\mu\text{m}$ , with a significant improvement at 1180  $\mu\text{m}$ .

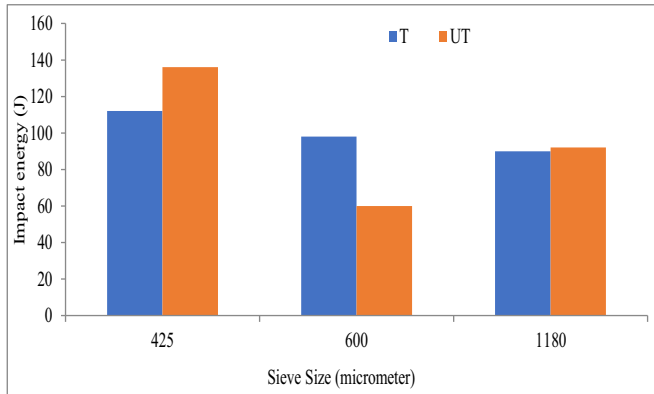


Figure 1: Impact energy properties for 5% RH reinforced composite

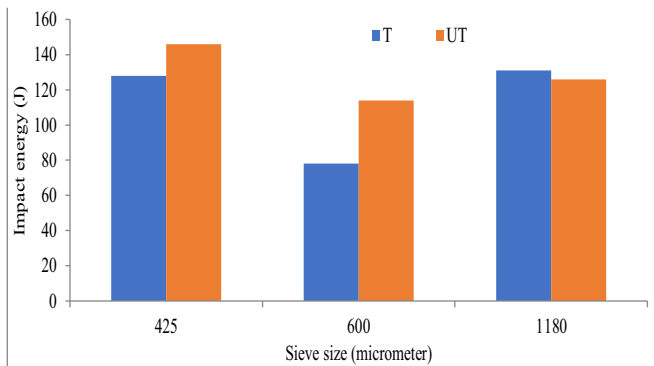


Figure 2: Impact energy properties for 10% RH reinforced composite

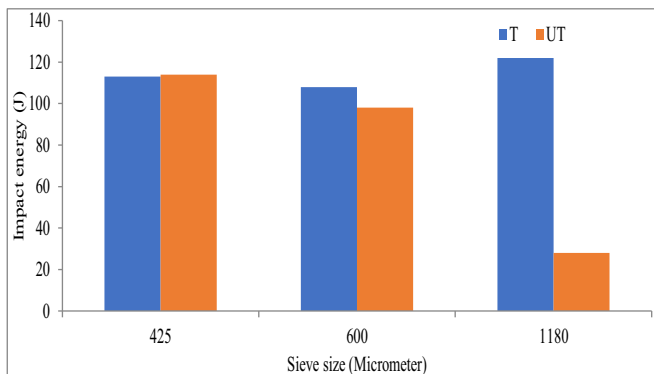


Figure 3: Impact energy properties for 10% coir/RH reinforced composite

Figures 4 and 5 reveal that treatment enhances water absorption at smaller particle sizes (425  $\mu\text{m}$  and 600  $\mu\text{m}$ ) but decreases it at larger ones (1180  $\mu\text{m}$ ). The study reveals that the treatment of RH composites impacts water absorption based on particle size, with the highest absorption at 425  $\mu\text{m}$  (13.46%). The study reveals that RH composite treatment affects water absorption based on particle size, with optimal particle size 425  $\mu\text{m}$  resulting in 13.46% water absorption. Figures 6 and 7 show water absorption percentages of treated and untreated coir composites at different particle sizes. Treated composites have higher water absorption percentages, with the highest value at 1180  $\mu\text{m}$  (18.51%). The highest value was observed at 1180  $\mu\text{m}$ , a significant increase from untreated composites (8.09%). The study shows that treatment significantly enhances water absorption in coir composites, with the highest percentage (18.51%) observed at 1180  $\mu\text{m}$ ,

compared to untreated composites.

Figure 8 shows that treating coir/RH composites improves water absorption at smaller particle sizes, but decreases at larger ones, suggesting durability and resistance to water exposure. Untreated composites at 600  $\mu\text{m}$  and 1180  $\mu\text{m}$  exhibit higher water absorption percentages, while treated composites have similar water absorption percentages. The graph reveals that treatment increases water absorption in treated coir/RH composites, with higher percentages observed at all particle sizes. The water absorption percentages varied with particle size, with the highest value at 600  $\mu\text{m}$  and the lowest at 425  $\mu\text{m}$ . Untreated composites had higher water absorption percentages at larger particle sizes, suggesting that treatment enhances water absorption.

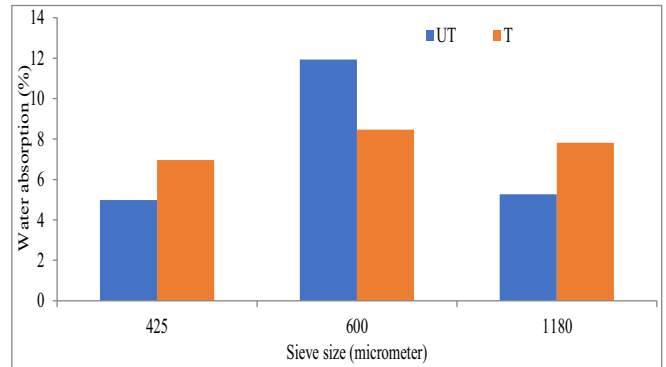


Figure 4: Water absorption properties for 5% RH reinforcement composite

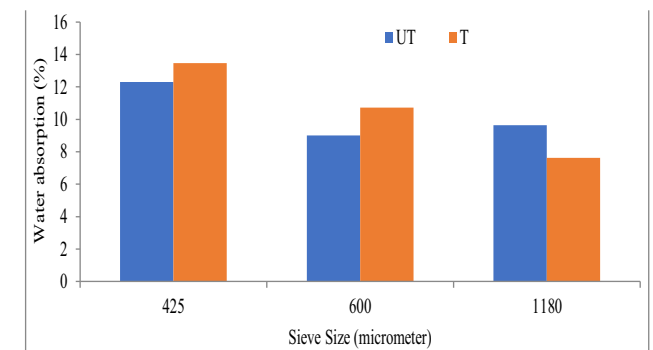


Figure 5: Water absorption properties for 10% RH reinforcement composite

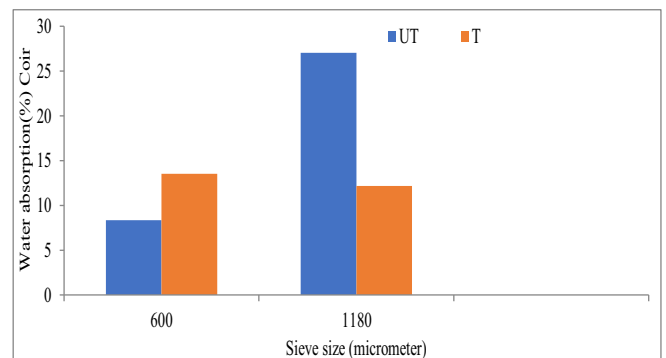


Figure 6: Water absorption properties for 5% coir reinforcement composite

The results of tests (Figure 6) reveal that treated RH composites exhibit higher water absorption at smaller particle sizes, while treated coir composites show higher absorption at all sizes, with a significant increase at 1180  $\mu\text{m}$  and a different trend at 600  $\mu\text{m}$ . Coir exhibits the highest water absorption in treated composites, followed by RH and coir/RH blend, indicating that material composition and treatment significantly influence composite water absorption properties.

TGA test evaluated samples' thermal stability, onset, endset, and organic waste residue, with results shown in Table 7. Onset temperature, the temperature at which transition begins, indicates better thermal stability as shown in Figures 9, 10, 11, 12 and 13. Samples with higher onset temperatures show better thermal stability, ranging from 85.4°C to 884.40°C. Endset temperature marks the end of

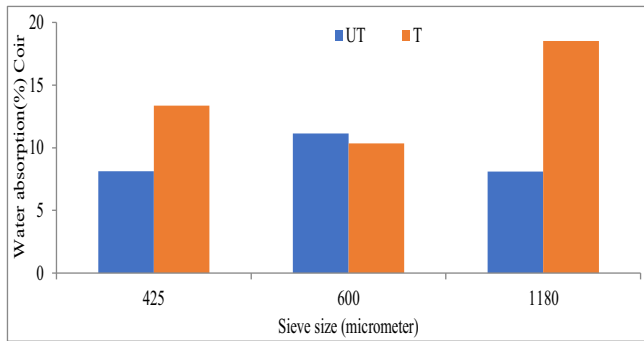


Figure 7: Water absorption properties for 10% coir reinforcement composite

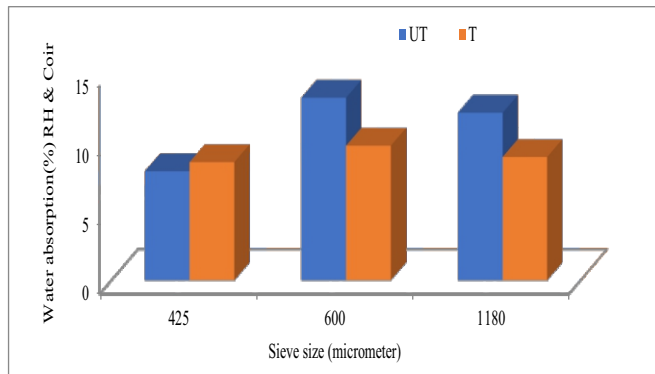


Figure 8: Water absorption properties for 10% coir/RH reinforcement composite

major decomposition, indicates the material's thermal stability, with higher endset temperatures indicating prolonged decomposition as shown in shown in Figures 10, 14, and 15 for 425  $\mu\text{m}$ , 600  $\mu\text{m}$ , and 1180  $\mu\text{m}$  respectively. The values range from 570.69°C to 889.69°C.

Figures 11, 16 and 17 analyzed the thermal decomposition of organic waste residues in samples, focusing on lower residue for thermal stability, with residue values ranging from 2.5% to 2.88%. Top samples for best thermal stability analysis indicates that samples with high onset and endset temperatures, lower organic waste residues, and high endset temperatures exhibit optimal thermal stability. These samples have low residue percentages, indicating effective decomposition and minimum remaining material left. The sample A4 (TRH 90/10) and sample F4 (URH 90/10) are deemed the most suitable for high thermal stability due to their overall performance (Table 7).

### 3.1 Surface Morphology of the Composite

SEM analysis examined the surface morphology and filler distribution of RH and coir fiber-reinforced epoxy composites. Images at 8000 $\times$  magnification were captured for treated and untreated coir, RH, and coir/RH composites with 10% filler reinforcement, as presented in Figures 18a to 19h.

#### 3.1.1 Particle size effect on surface morphology of the composite samples

Surface morphology of smaller particles is smoother, while larger particles become rougher and rougher as illustrated in Figures 18a to 18h. Larger particle sizes have poor adhesion between fillers and epoxy matrix, causing stress concentration and fracture initiation, as reported by Khalid et al., (2021).

3.1.2 Chemical treatment effect on surface morphology of the composite samples  
SEM images of treated samples for RH, coir, and RH/coir fillers composites show smoother surfaces compared to untreated samples. Chemical treatment improves adhesion between filler particles and epoxy matrix by removing waxes and lignin on lignocellulosic fiber surfaces as illustrated in Figures 19a to 19h.

Table 7: TGA data test results

	Sample	Name	Temp (°C)	Total wt loss (%)	Heat capacity generated j/g	Heat capacity generated (mj)	Organic waste residue (%)	Onset temp	Endset temp
1	A0	Control	99.9	99.8	4.85	282.62	2.40	874.40	789.49
2	A2	TC 90/10	99.9	99.5	4.85	152.62	2.77	884.40	689.69
3	A4	TRH 90/10	99.9	99.8	4.85	2586.45	2.80	834.40	889.69
4	A6	TRHC 90/10	99.9	99.9	4.85	282.62	2.70	85.40	789.89
5	B2	TC 90/10	99.9	99.8	4.85	282.62	2.50	850.20	799.40
6	B4	TRH 90/10	99.9	99.5	4.85	152.62	2.65	884.40	689.69
7	C2	TC 90/10	99.9	99.8	4.64	262.02	2.80	877.30	772.60
8	C4	TRH 90/10	99.9	99.5	4.85	152.62	2.65	784.40	689.69
9	C6	TRHC90/10	99.9	99.7	4.85	2586.45	2.80	834.40	789.69
10	D2	UC 90/10	100	99.8	4.85	282.62	2.70	874.40	789.40
11	D4	URH 90/10	99.9	99.9	4.90	250.22	2.68	684.40	570.69
12	D6	URHC 90/10	99.9	99.5	4.85	152.62	2.80	880.70	789.69
13	E2	UC 90/10	99.9	98.9	4.90	250.22	2.88	684.40	570.69
14	E4	URH 90/10	99.9	99.5	4.85	152.62	2.80	880.70	789.69
15	F2	UC 90/10	99.9	99.5	4.85	152.62	2.77	884.40	689.69
16	F4	URH 90/10	99.9	99.8	4.85	2586.45	2.80	834.40	889.69
17	F6	URHC 90/10	99.9	99.9	4.85	282.62	2.70	85.40	789.89

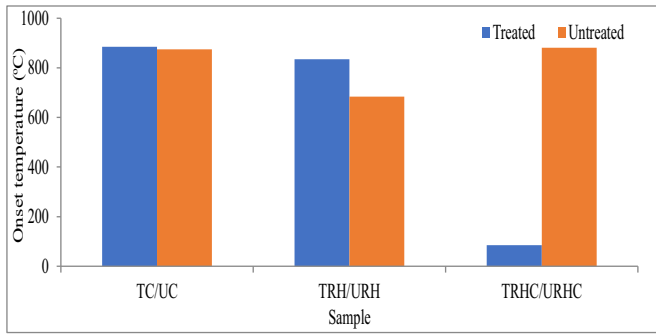


Figure 9: Onset temperature of sieve size 425 µm for treated and untreated composite

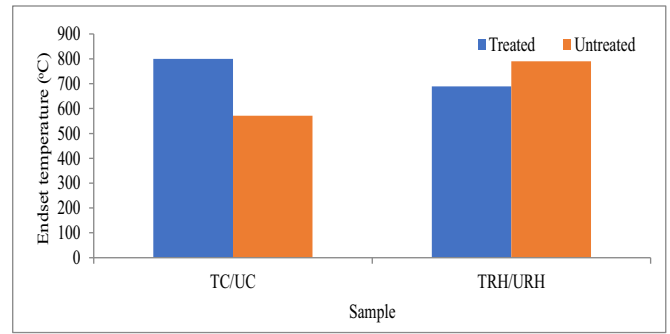


Figure 13: Endset temperature of sieve size 600 µm for treated and untreated composite

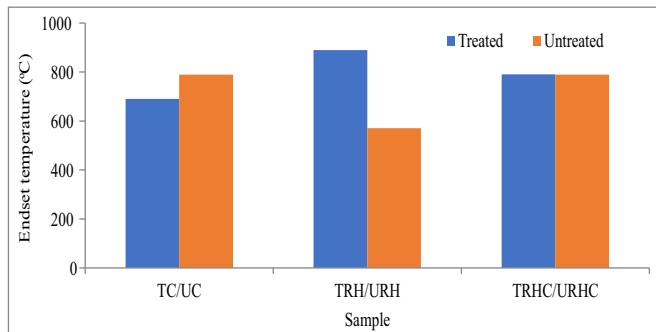


Figure 10: Endset temperature of sieve size 425 µm for treated and untreated composite

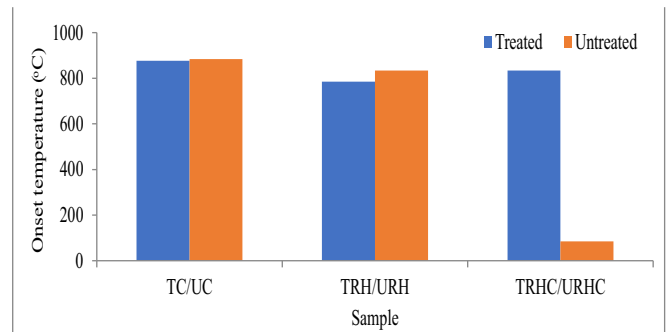


Figure 14: Onset temperature of sieve size 1180 µm for treated and untreated composite

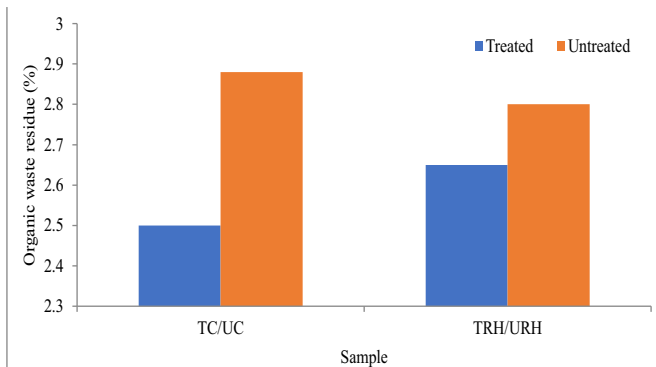


Figure 11: Organic waste residue of sieve size 600 µm for treated and untreated composite

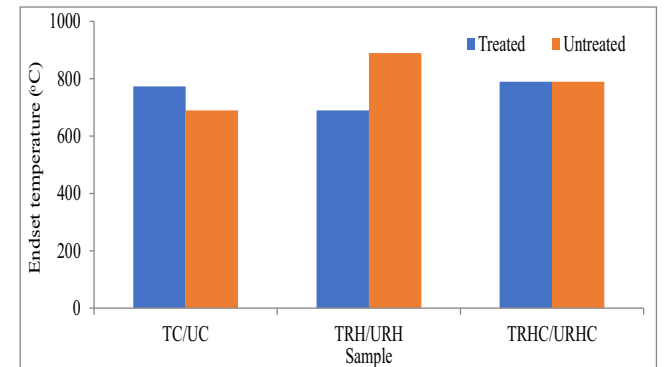


Figure 15: Endset temperature of sieve size 1180 µm for treated and untreated composite

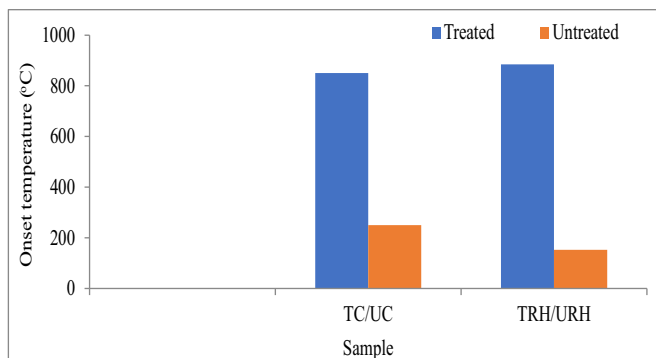


Figure 12: Onset temperature of sieve size 600 µm for treated and untreated composite

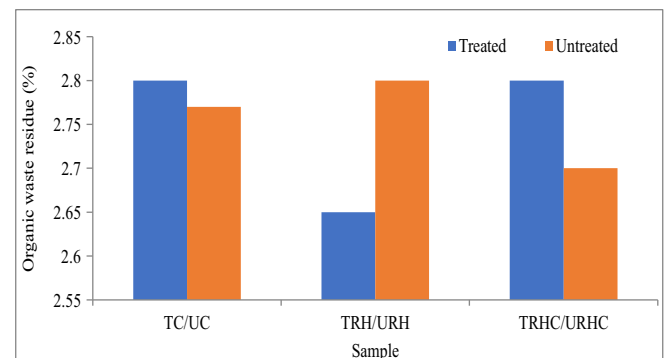


Figure 16: Organic waste residue of sieve size 1180 µm for treated and untreated composite



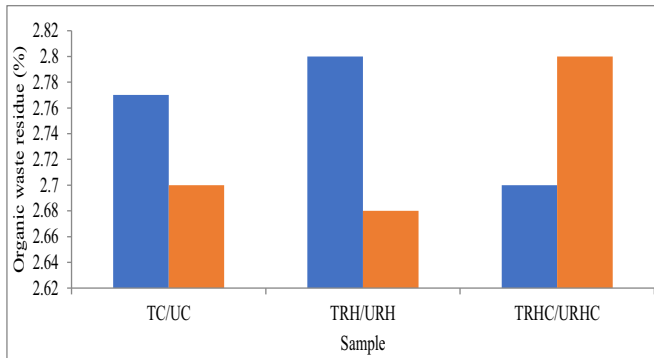


Figure 17: Organic waste residue of sieve size 425  $\mu\text{m}$  for treated and untreated composite

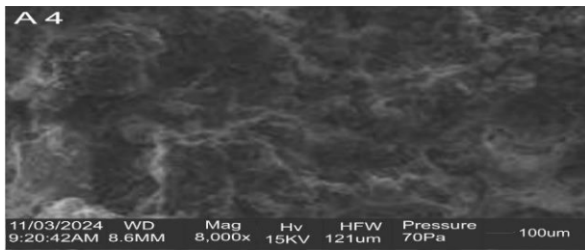


Figure18a: SEM image of TC 10% filler of 425  $\mu\text{m}$ size

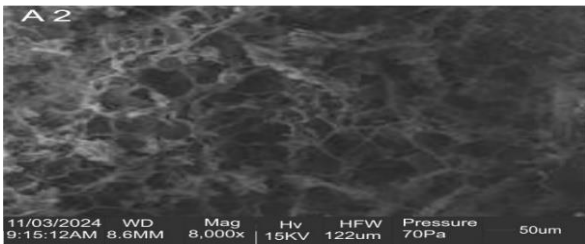


Figure18b: SEM image of TRH 10% filler of 425  $\mu\text{m}$  size

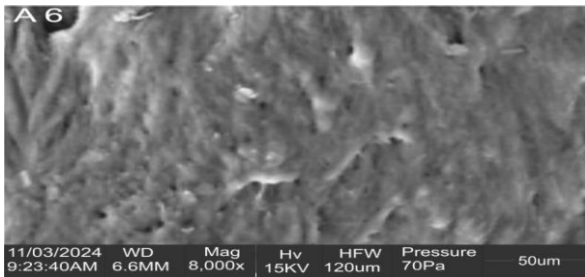


Figure18c: SEM image of TCRH 10% filler of 425  $\mu\text{m}$ size

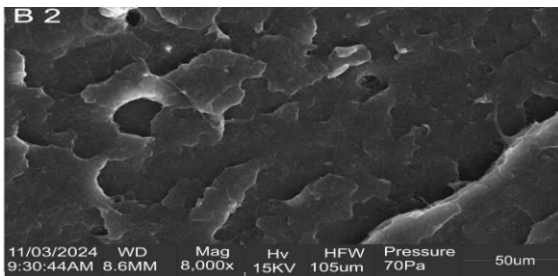


Figure18d: SEM image of TC 10% filler of 600  $\mu\text{m}$  size

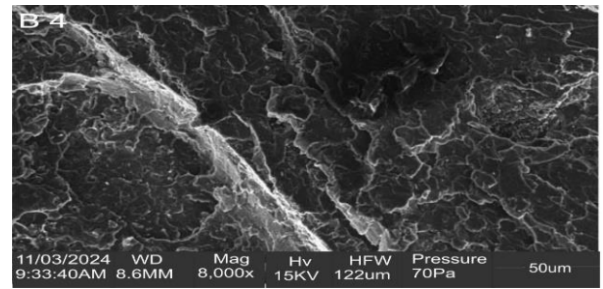


Figure18e: SEM image of TRH 10% filler of 600  $\mu\text{m}$  size

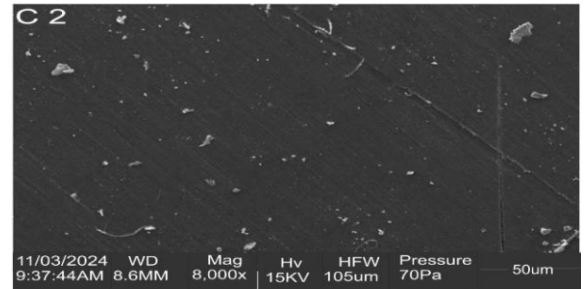


Figure18f: SEM image of TC 10% filler of 1180  $\mu\text{m}$  size

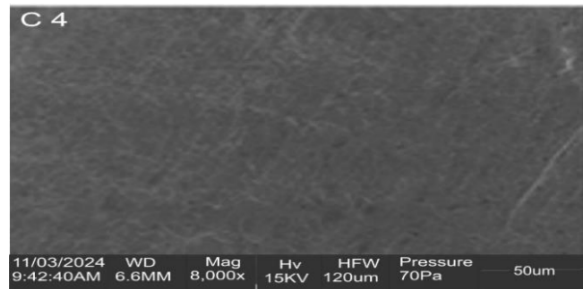


Figure18g: SEM image of TRH 10% filler of 1180  $\mu\text{m}$  size

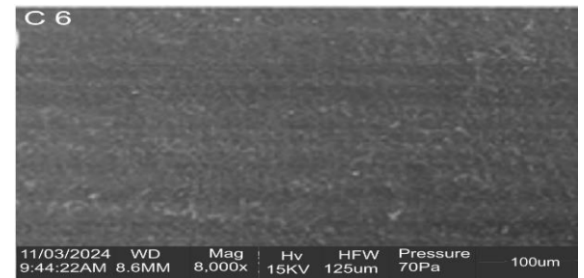


Figure18h: SEM image of TCRH 10% filler of 425  $\mu\text{m}$  size

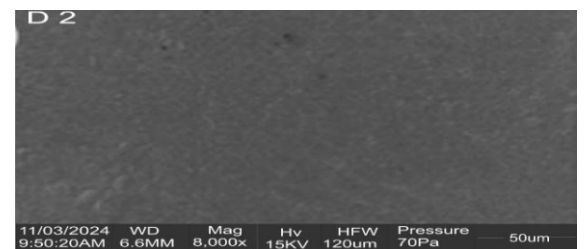
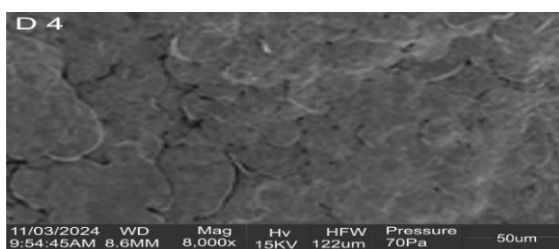
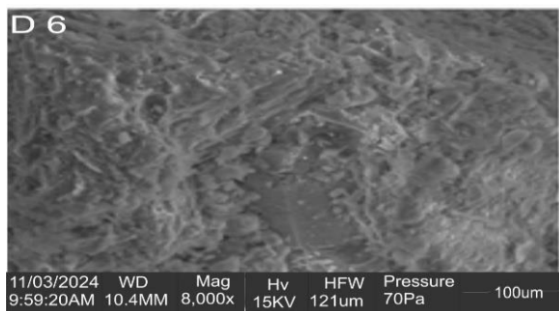
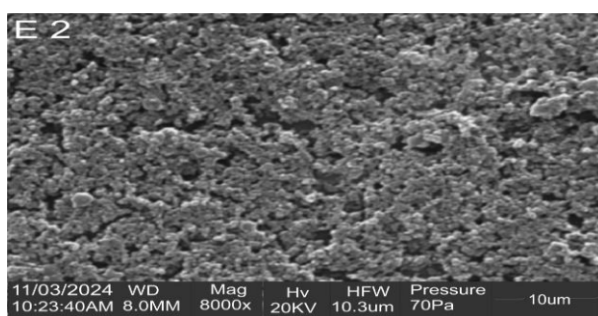
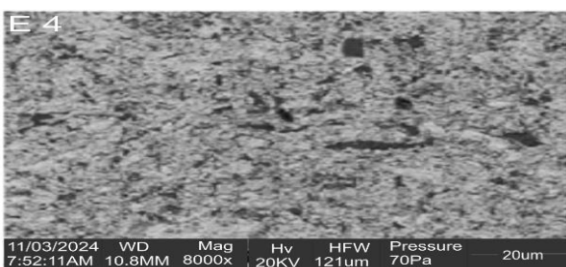
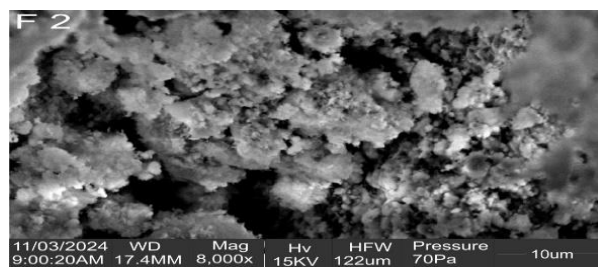
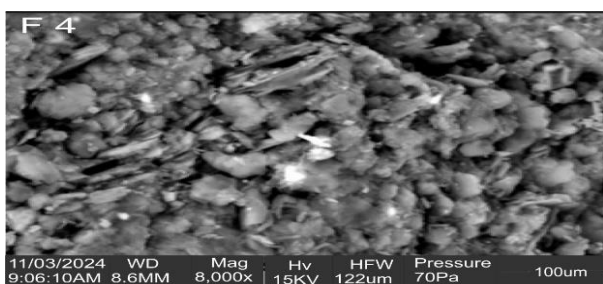
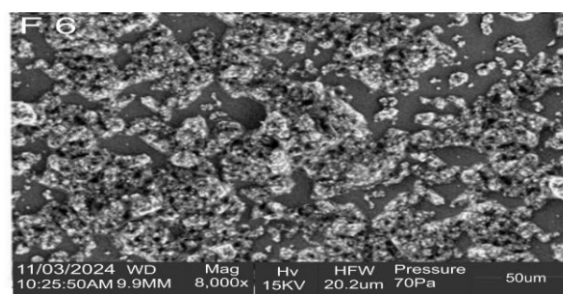


Figure19a: SEM image of UTC 10% filler of 425  $\mu\text{m}$  size

Figure19b: SEM image of UTRH 10% filler of 425  $\mu\text{m}$  sizeFigure19c: SEM image of UTRH 10% filler of 425  $\mu\text{m}$  sizeFigure19d: SEM image of UTC 10% filler of 600  $\mu\text{m}$  sizeFigure19e: SEM image of URH 10% filler of 600  $\mu\text{m}$  sizeFigure19f: SEM image of UTC 10% filler of 1180  $\mu\text{m}$  sizeFigure19g: SEM image of UTRH 10% filler of 1180  $\mu\text{m}$  sizeFigure19h: SEM image of UTRH 10% filler of 41180  $\mu\text{m}$  size

#### 4. Conclusion

The study investigates the mechanical properties of coir fibres and rice husks, their potential use in sustainable automotive dashboards, and the impact of particle size and treatment. The research examined the mechanical, thermal, and water absorption properties of coir fibre and rice husk-reinforced epoxy composites, using thermogravimetric analysis, Fourier Transform Infrared Spectrometry, Scanning Electron Microscope, and Izod impact testing to assess their impact resistance and thermal stability. Rice husk composites exhibit increased water absorption at smaller particle sizes, while coir composites show enhanced absorption at larger sizes. Coir/RH blends maintain consistent water absorption, while untreated composites show higher impact energy. The study suggests using smaller particle sizes (425  $\mu\text{m}$ ) and untreated coir for the reinforcement of epoxy composites, with the optimal size for treated composites being 1180  $\mu\text{m}$ . Heat treatment and particle size significantly affect mechanical and water absorption properties.

#### References

- Abhishek T.H. and Mrutyunjaya G. (2016). Evaluation of mechanical and water absorption behaviour of coir and rice husk reinforced composites: International Journal of Research in Engineering and Technology, 5(3), 77-85
- Ahmed, H., Noyon, M.A., Uddin, M.E., Jamal, M., and Palaniappan, S.K. (2023). Biodegradable and flexible fiber-reinforced composite sheet from tannery solid wastes: an approach of waste minimization. Polymer Composites, 44(11), 7545-7556. <https://doi.org/10.1002/pc.27644>.
- Akter, M., Uddin, M.H., and Anik, H.R. (2024). Plant fiber-reinforced polymer composites: a review on modification, fabrication, properties, and applications. Polymer Bulletin, 81(1), 1-85. <https://doi.org/10.1007/s00289-023-04733-5>.
- Chichane, A., Boujmal, R., and El-Barkany, A. (2023). Bio-composites and bio-hybrid composites are reinforced with natural fibers. Materials Today: Proceedings, 72, 3471-3479. <https://doi.org/10.1016/j.matpr.2022.08.132>.
- Choi, J.Y., Jeon, J.H., Lyu, J.H., Park, J., Kim, G.Y., Chey, S.Y., Quan, Y.J., Bhandari, B., Prusty, B.G., and Ahn, S.H. (2023). Current applications and development of composite manufacturing processes for future mobility. International Journal of Precision Engineering and Manufacturing-Green Technology, 10(1), 269-291. <https://doi.org/10.1007/s40684-022-00483-3>.
- Faheed, N.K. (2024). Advantages of natural fiber composites for biomedical applications: a review of recent advances. Emergent Materials, 7, 63-75. <https://doi.org/10.1007/s42247-023-00620-x>.
- Ganasan, V., Chohan, J.S., Subburaj, G.S., Harika, K., Yedari, V., Sivakumar, N.S., Raheena, S., and Durai, A.J. (2024). Mechanical, moisture absorption, and thermal stability of banana fiber/eggshell powder-based epoxy composites. Engineering Proceedings, 61(1), 11. <https://doi.org/10.3390/engproc2024061011>.
- Gil-Sánchez H.H., Zuleta-Gil A. A., Reyes-Campo D. E. (2021). Mechanical properties and sustainability aspects of coconut fiber-modified concrete. Artículo de investigación científica y tecnológica, Scientia et Technica Año XXVI, 26(01) DOI: <https://doi.org/10.22517/23447214.22901>
- Khalid, M.Y., Al Rashid, A., Arif, Z.U., Ahmed, W., Arshad, H., and Zaidi, A.A. (2021). Natural fiber-reinforced composites: Sustainable materials for emerging applications. Results in Engineering, 11, 100263. <https://doi.org/10.1016/j.rineng.2021.100263>.
- Kiruthika, A.V. (2024). A review of leaf fiber-reinforced polymer composites. Journal of Engineering and Applied Science, 71(24), 1-31. <https://doi.org/10.1186/s44147-024-00365-2>.
- Mohan, T.P. and Kannu, K. (2023). Dynamic mechanical analysis of glass fiber-reinforced epoxy-filled nanoclay hybrid composites. Materials Today: Proceedings, 87(1), 235-245. <https://doi.org/10.1016/j.matpr.2023.05.282>.
- Nasri, W., Djebali, R., Chamkha, A.J., Bezazi, A., Mechighel, F., Reis, P., and Driss, Z. (2024). Thermal behavior of mesoporous aramid fiber-reinforced silica aerogel composite for thermal insulation applications: microscale

- modeling. *Journal of Applied and Computational Mechanics*, 10(1), 140-151. <https://doi.org/10.22055/jacm.2023.44601.4247>.
- Oyiborhoro, G., Anegebe, B., Odiachi, I.J., Atoe, B., and Ifijen, I.H. (2024). Environmental impact of multi-component fiber-reinforced composites: challenges and green solutions. *The Minerals, Metals, and Materials Series*, 6(2), 1237-1252. [https://doi.org/10.1007/978-3-031-50349-8\\_107](https://doi.org/10.1007/978-3-031-50349-8_107)
- Patel, M., Pardhi, B., Chopara, S., and Pal, M. (2018). Lightweight composite materials for automotive: a review. *International Research Journal of Engineering and Technology*, 5(11), 41-47.
- Sakti P.S. (2014). Tribological behavior of rice husk-reinforced polymer matrix composite: a thesis submitted in partial fulfillment of the requirement for the degree of doctor of philosophy, Department of Mechanical Engineering, National Institute of Technology Rourkela—769 008, (India).
- Sanjay, M.R., Arpitha, G.R., Naik, L.L., Gopalakrishna, K., and Yogesha, B. (2016). Applications of natural fibers and their composites: an overview. *Natural Resources*, 7, 108-114.
- Santos, T.F., Santos, C.M., Aquino, M.S., Suyambulingam, I., Kamil Hussein, E., Verma, A., Rangappa, S.M., Siengchin, S., and Nascimento, J.H. (2024). Towards sustainable and eco-friendly polymer composite materials from bast fibers: a systematic review. *Engineering Research Express*. <https://doi.org/10.1088/2631-8695/ad2640>.
- Shaaban, S., El-Abden, S.Z., and Ali, W.Y. (2024). Electrostatic charge generated from the sliding of rubber on epoxy filled by natural fibers. *Journal of the Egyptian Society of Tribology*, 21(1), 120-133. <https://doi.org/10.21608/JEST.2024.336522>.
- Sharma, S., Sudhakara, P., Misra, S.K., and Singh, J. (2020). A comprehensive review of current developments on the waste-reinforced polymer-matrix composites for automotive, sports goods, and construction applications: Materials, processes, and properties. *Materials Today: Proceedings*, 33, 1671-1679. <https://doi.org/10.1016/j.matpr.2020.06.523>.
- Umma, A. (2022). Utilization and mechanical properties of rice husk as useful agro-waste and reinforcement in composites fabrication: a critical review: *African Journal of Engineering and Environment Research*. 3(2), 2635-2974.
- Valasek, P., Müller, M., Sleger, V., Kolar, V., Hromasova, M., D'Amato, R., and Ruggiero, A. (2021). Influence of alkali treatment on the microstructure and mechanical properties of coir and abaca fibers. *Materials*. 14, 26-36.
- Wang, S., Zheng, Z., Long, J., Wang, J., Zheng, K., Ke, Z., Luo, Z., Pokrovsky, A.I., and Khina, B.B. (2024). Recent advances in wear-resistant steel matrix composites: a review of reinforcement particle selection and preparation processes. *Journal of Materials Research and Technology*, 29, 1779-1797. <https://doi.org/10.1016/j.jmrt.2024.01.195>.